

# A Theoretical Approach for Computing Magnetic Anisotropy in Single Molecule Magnets

Rajamani Raghunathan<sup>§</sup>, S. Ramasesha<sup>§</sup> and Diptiman Sen<sup>#</sup>

<sup>§</sup>*Solid State and Structural Chemistry Unit, Indian Institute of Science, Bangalore 560012. INDIA.*

<sup>#</sup>*Centre for High Energy Physics, Indian Institute of Science, Bangalore 560012. INDIA.\**

(Dated: June 3, 2008)

We present a theoretical approach to calculate the molecular magnetic anisotropy parameters,  $D_M$  and  $E_M$  for single molecule magnets in any eigenstate of the exchange Hamiltonian, treating the anisotropy Hamiltonian as a perturbation. Neglecting inter-site dipolar interactions, we calculate molecular magnetic anisotropy in a given total spin state from the known single-ion anisotropies of the transition metal centers. The method is applied to  $Mn_{12}Ac$  and  $Fe_8$  in their ground and first few excited eigenstates, as an illustration. We have also studied the effect of orientation of local anisotropies on the molecular anisotropy in various eigenstates of the exchange Hamiltonian. We find that, in case of  $Mn_{12}Ac$ , the molecular anisotropy depends strongly on the orientation of the local anisotropies and the spin of the state. The  $D_M$  value of  $Mn_{12}Ac$  is almost independent of the orientation of the local anisotropy of the core  $Mn(IV)$  ions. In the case of  $Fe_8$ , the dependence of molecular anisotropy on the spin of the state in question is weaker.

PACS numbers: 75.50.Xx, 75.30.Gw

## I. INTRODUCTION

Following the synthesis and the discovery of exotic properties such as quantum resonant tunneling (QRT) in the single molecule magnet (SMM)  $Mn_{12}Ac$  during the 1990s, there has been a flurry of activity in the field of molecular magnetism [1, 2, 3, 4]. This has led to the synthesis of new systems such as  $Fe_8$  as well as to the observation of new phenomena such as quantum coherence [5, 6]. SMMs are mainly high nuclearity transition metal complexes with a high-spin ground state ( $S_{GS}$ ). They are also characterized by large uniaxial magnetic anisotropy [7]. The Hamiltonian corresponding to the magnetic anisotropy of a molecular system can be written as,

$$\hat{H}_D = \hat{S}_M \cdot \mathcal{D}^{(M)} \cdot \hat{S}_M \quad (1)$$

where,  $\hat{S}_M$  is the spin operator for the total spin of the molecule and  $\mathcal{D}^{(M)}$  is the magnetic anisotropy tensor of the molecule. In usual practice, the anisotropy tensor is diagonalized and the principle axis of the molecule would correspond to the eigenvectors of the tensor. Since in most physical situations, the quantity of interest is the energy gaps between the otherwise degenerate states split by the magnetic anisotropy, the condition of zero trace is imposed on the  $\mathcal{D}^{(M)}$  tensor. If,  $D_{XX}^M$ ,  $D_{YY}^M$  and  $D_{ZZ}^M$  are the molecular anisotropies along the three principal directions such that  $D_{XX}^M + D_{YY}^M + D_{ZZ}^M = 0$ , we can define two parameters,  $D_M$  and  $E_M$  given by,

$$\begin{aligned} D_M &= D_{ZZ}^M - \frac{1}{2} (D_{XX}^M + D_{YY}^M) \\ E_M &= \frac{1}{2} (D_{XX}^M - D_{YY}^M) \end{aligned}$$

where,  $D_M$  and  $E_M$  are called the axial and rhombic anisotropies respectively. This leads to the common form of the magnetic anisotropy Hamiltonian of a SMM,

$$\hat{H}_M = D_M \left( \hat{S}_Z^2 - \frac{1}{3} S(S+1) \right) + E_M \left( \hat{S}_X^2 - \hat{S}_Y^2 \right) \quad (2)$$

For the single molecule magnet to have nonzero magnetization in the ground state, it is necessary that the anisotropy constant  $D_M$  in the spin Hamiltonian (Eq. 2) of the complex be negative; this ensures that the ground state of the system then would correspond to the highest magnetization state of the molecule, in its high-spin ground state. This requirement of negative  $D_M$ , besides a high-spin ground state makes it hard to tailor SMMs. The second order transverse or rhombic anisotropy given by the last term in Eq. 2, allows transition between states with spin  $S$  that differ in their  $M_s$  values by two.  $E_M$  will be zero if the  $\hat{S}_X^2 - \hat{S}_Y^2$  operator does not remain invariant under symmetry of the molecule. In this case higher order spin-spin interaction terms are required to observe QRT. For example, the  $D_{2d}$  symmetry in  $Mn_{12}Ac$  prohibits the existence of first order rhombic anisotropy. Thus, the parameters  $D_M$  and  $E_M$  govern the quantum tunneling properties of a SMM and inputs from theoretical modeling could help in designing the architecture for the synthesis of SMMs.

Theoretical modeling of SMMs presents two difficulties. Firstly, the complexes contain many spin centers, and often these centers have different spins as in the case of  $Mn_{12}Ac$ , where the four  $Mn(IV)$  ions have spin-3/2, while the eight  $Mn(III)$  ions have spin-2. In these systems, usually there exist multiple exchange pathways between any given pair of ions leading to uncertain magnitude and sign of the magnetic interactions in the system. The topology of magnetic interactions also is often such as to result in magnetic frustration leading to closely spaced low-lying states of unpredictable total spin. Thus,

\*Electronic address: ramasesh@sscu.iisc.ernet.in

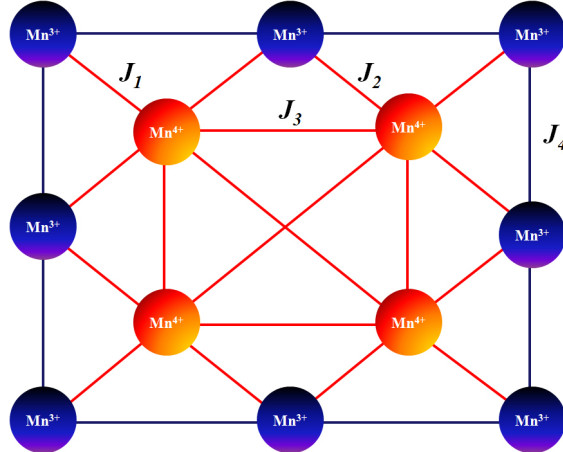


FIG. 1: Schematic of possible exchange interactions in  $Mn_{12}Ac$  SMM. The peripheral  $Mn(III)$  ions represented by blue circles correspond to spin-2 sites and those represented by yellow circles are the core  $Mn(IV)$  ions each of spin-3/2.  $J$ s are the strength of superexchange interaction with  $J_1=215$  K,  $J_2=J_3=85.6$  K,  $J_4=-64.5$  K [9].

solving even the simple Heisenberg exchange Hamiltonian of these systems turns out to be a challenge. If we do not employ a spin adapted basis to set-up the Hamiltonian matrix we could encounter convergence difficulties associated with closely spaced eigenvalues even when the corresponding eigenstates belong to different total spin sectors. However, the assorted spin cluster that a SMM is renders construction of spin adapted basis difficult. This problem has been addressed by resorting to a valence bond scheme for construction of the spin adapted basis and we are now in a position to block-diagonalize the Hamiltonian by exploiting both spin and spatial symmetries [8]. Thus, while the challenge of accurately solving the exchange Hamiltonian of a large assorted spin system with arbitrary topology of exchange interactions is within grasp, the challenge of computing the magnetic anisotropy constants of a SMM still remains.

The magnetic anisotropy in an isolated ion arises from explicit dipolar interactions between the unpaired electrons in the magnetic center as well as from relativistic (spin-orbit) interactions. The former is the main origin of zero field splitting observed in triplet states of conjugated organic molecules such as naphthalene [10]. However, in systems containing heavier elements the relativistic effects dominate. In a system with several magnetic centers such as a SMM, given the spin and single ion anisotropy of each magnetic center, the magnetic anisotropy could arise both from dipolar interactions between magnetic centers and relativistic effects. Theoretically, magnetic anisotropy of an isolated magnetic center in an appropriate ligand environment can be computed within density functional techniques (DFT) [11, 12]. However, in the case of the SMMs with many magnetic centers, such a calculation is both conceptually and computationally difficult, since DFT methods

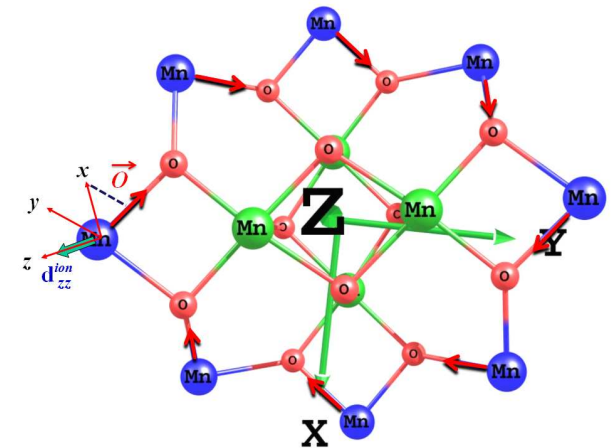


FIG. 2: Schematic of local ( $x, y, z$ ) and laboratory ( $X, Y, Z$ ) coordinate axes in  $Mn_{12}Ac$ . The blue, green and red spheres correspond to  $Mn(III)$  (spin-2),  $Mn(IV)$  (spin-3/2) and oxygen ions respectively. The arrows indicate the  $Mn-O$  bonds on which the chosen local  $x$ -axis has maximum projection.

do not conserve total spin. The usual approach in these cases is to carry out simple tensoral summation of the anisotropies of the constituent magnetic centers to obtain the magnetic anisotropy in the SMMs along the lines of an oriented gas model employed in the calculation of macroscopic nonlinear optic (NLO) coefficients from isolated molecular NLO coefficients [13, 14, 15]. Such an approach, in the case of SMMs, suffers from the drawback that the anisotropy constants so computed are independent of the total spin state of the molecule. In this paper, we treat the anisotropic magnetic interaction between the magnetic centers as a perturbation over the magnetic exchange Hamiltonian of the SMM. We exactly solve for the various total spin states of the unperturbed Hamiltonian and from the desired eigenstates obtain the spin-spin correlation functions necessary to compute the anisotropy constants. In the next section we describe the method in detail. In the third section we present the results of our studies on the two SMMs,  $Mn_{12}Ac$  and  $Fe_8$ . In the fourth section we summarize our studies and outline the extension of this method for the computation of higher order magnetic anisotropy constants.

## II. FORMULATION OF THE METHOD

We treat the exchange Hamiltonian between magnetic centers in the SMMs as the unperturbed Hamiltonian,

$$\hat{H}_0 = \sum_{\langle ij \rangle} J_{ij} \hat{S}_i \cdot \hat{S}_j \quad (3)$$

where,  $\langle ij \rangle$  runs over all pairs of centers in the model for which the exchange constant is nonzero,  $\hat{S}_i$  is the spin on the  $i$ th magnetic center. In SMMs such as  $Mn_{12}Ac$  the spins at all the magnetic centers are not the same and

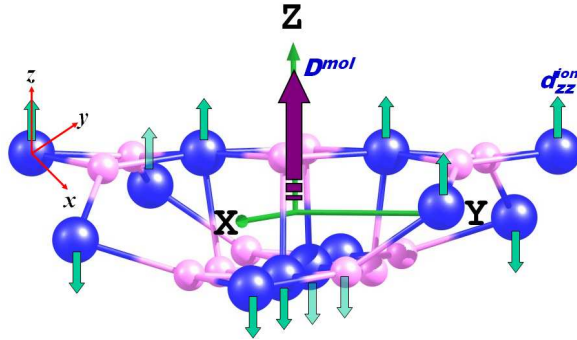


FIG. 3: Schematic diagram showing the directions of local anisotropy in  $Mn_{12}Ac$ . The single-ion anisotropies of all the Mn ions are directed along the laboratory  $Z$  axis (Scheme 1).

the exchange interactions are shown in Fig. 1.  $H_0$  can be solved exactly for a few low-lying states in a chosen spin sector by using methods that have been described in detail elsewhere [9].

The general anisotropic interactions in a collection of magnetic centers is treated as a perturbation with Hamiltonian  $\hat{H}'_1$  is given by,

$$\hat{H}'_1 = \frac{1}{2} \sum_i \sum_j \sum_{\alpha} \sum_{\beta} D_{ij,\alpha\beta} \hat{S}_i^{\alpha} \hat{S}_j^{\beta} \quad (4)$$

where, the indices  $i$  and  $j$  run over all the magnetic centers and  $\alpha$  and  $\beta$  run over  $x$ ,  $y$  and  $z$  directions of the ion. The contributions to inter-center anisotropy constant arise due to dipolar interaction between the spins on the two centers as well as due to relativistic effects. In the former,  $D_{ij,\alpha\beta}$  is given by,

$$D_{ij,\alpha\beta} = \frac{1}{2} g^2 \mu_B^2 \left\langle \frac{\mathcal{R}_{ij}^2 \delta_{\alpha\beta} - 3R_{ij,\alpha} R_{ij,\beta}}{R_{ij}^5} \right\rangle \quad (5)$$

where  $\mathcal{R}_{ij}$  ( $R_{ij}$ ) is the vector (distance) between the magnetic centers  $i$  and  $j$ ,  $g$  is the gyromagnetic ratio and  $\mu_B$  is the electronic Bohr magneton; the expectation value in Eq. 5 is obtained by integration over spatial coordinates [16]. Approximating the expectation values of the distances by the equilibrium distances, the  $D_{ij,\alpha\beta}$  in Eq. 5 and by computing the necessary spin-spin correlation functions, we can obtain the molecular  $\mathcal{D}_{\alpha\beta}^{(M)}$  tensor [17]. The eigenvalues of this matrix give the principal anisotropy values and imposing the condition of zero trace of the matrix yields molecular magnetic anisotropy constants due to spin-spin interactions. Our computation of the magnetic anisotropy constants, assuming only spin dipolar interactions for the SMMs  $Mn_{12}Ac$  and  $Fe_8$  gives negligible values of the anisotropy constants compared to the experimental values of  $D_M = -0.7$  K and  $-0.28$  K respectively in the  $S=10$  ground state [18, 19]. Hence in what follows, we completely neglect the contribution of spin-dipolar interactions and focus only on the magnetic anisotropy of the SMMs arising from the anisotropy of individual magnetic centers. The latter is a consequence of

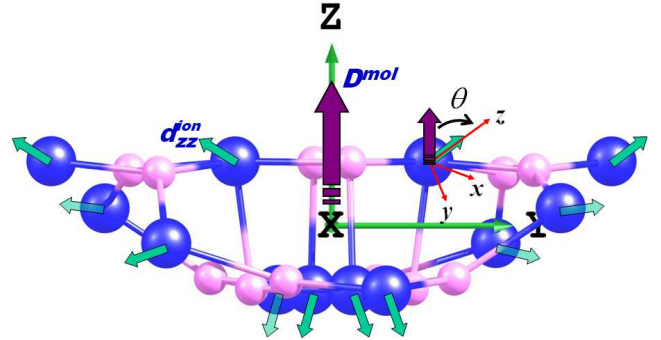


FIG. 4: Schematic diagram showing the directions of local anisotropy in  $Mn_{12}Ac$ . The  $z$ -component of the single-ion anisotropies of all the Mn(III) ions are inclined at an angle  $\theta$  to the laboratory  $Z$  and while that of the Mn(IV) ions are kept fixed at  $\sim 48^\circ$  (Scheme 2).

mainly spin-orbit interactions. We now assume that the interactions responsible for magnetic anisotropy are short ranged and neglect inter-center contributions to magnetic anisotropy in Eq. 4. This is justified since relativistic (spin-orbit) interactions, largely responsible for the anisotropy is short ranged (falling off as  $1/r^3$ ) and the distances between the magnetic centers is much larger compared to the ionic radius of the transition metal ion. The resulting perturbation term is given by,

$$\hat{H}_1 = \sum_i \sum_{\alpha} \sum_{\beta} D_{i,\alpha\beta} \hat{S}_i^{\alpha} \hat{S}_i^{\beta} \quad (6)$$

where, only on-site terms are retained. If the individual magnetic centers have different principal axes then we choose a laboratory frame and project the local tensor components on to the laboratory frame. In such a case, Eq. 6 gets modified to,

$$\hat{H}_1 = \sum_i \sum_{\alpha} \sum_{\beta} \sum_l \sum_m C_{i,l\alpha} C_{i,m\beta} D_{i,\alpha\beta} \hat{S}_i^{\alpha} \hat{S}_i^{\beta} \quad (7)$$

Where,  $C_{i,l\alpha}$  are the direction cosines of the local axis of the  $i$ th magnetic center with the  $l(m)$  being the coordinate of the laboratory frame and  $\alpha(\beta)$  being the local coordinates. Since, the Hamiltonians in Eq. 1 and 7 are equivalent, we can equate the matrix elements  $\langle n, S_M, M | \hat{H}_1 | n, S_M, M' \rangle$  and  $\langle S_M, M | \hat{H}_M | S_M, M' \rangle$  for any pair of eigenstates of the exchange Hamiltonian in Eq. 3;  $|M\rangle$  and  $|M'\rangle$  correspond to a state  $n$  with spin  $S_M$  in which we are interested. Calculating these matrix elements for  $\hat{H}_M$  is straightforward from the algebra of spin operators. However, evaluation of these matrix elements between eigenstates of  $\hat{H}_0$ , requires computing them in the basis of the spin orientation of the sites. From a given eigenstate of  $\hat{H}_0$ ,  $|n, S, M\rangle$ , we can compute all eigenstates with different  $M$  values by using ladder operators corresponding to spin  $S$ . Given a  $S$  value, the above condition would give rise to  $(2S + 1)^2$  equations, while the tensor  $\mathcal{D}^{(M)}$ , has only nine components. Thus, for

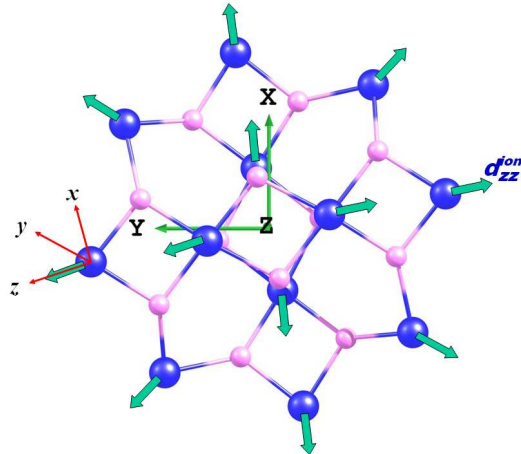


FIG. 5: Schematic diagram showing the directions of local anisotropy in  $Mn_{12}Ac$ . The  $z$ -component of the single-ion anisotropies of all the  $Mn$  ions are directed along the plane perpendicular to the laboratory  $Z$  axis (Scheme 3).

the  $Mn_{12}Ac$  system, with ground state spin of 10, there would be 441 equations and we have more equations than unknowns. However, we could take any nine equations and solve for the components of the tensor  $\mathcal{D}^{(M)}$  and we would get unique values of the components. This is guaranteed by the Wigner-Eckart theorem and we have also verified this by solving for the  $\mathcal{D}^{(M)}$  tensor from several arbitrarily different selections of the nine equations.

### III. RESULTS AND DISCUSSION

We have computed  $D_M$  and  $E_M$  values for both  $Mn_{12}Ac$  and  $Fe_8$  systems for different orientations of local anisotropy. We have used the single-ion anisotropy values quoted in the literature for complexes of these ions in similar ligand environments [20, 21, 22, 23]. While discussing the results, we refer to the local axis of the ions as  $x$ ,  $y$  and  $z$  and the laboratory axis is denoted as  $X$ ,  $Y$  and  $Z$ . The laboratory frame we choose can be arbitrary. This is because, on determining  $\mathcal{D}^{(M)}$  in the laboratory frame, we diagonalize it and the principal axis of the molecule is given by the eigenvectors of the  $\mathcal{D}^{(M)}$  matrix. The principal axes of the molecule are unique and do not depend on the laboratory frame that is selected. We have computed the anisotropy parameters for both these systems as a function of the angle  $\theta$  which the  $z$ -axis of the ion makes with the laboratory  $Z$ -axis. The orientation of  $z$ -component of the single-ion anisotropy in every site is shown in Fig. 3, 4 and 5 (schemes 1, 2 and 3) for  $Mn_{12}Ac$  and in Fig. 8, 9, and 10 (schemes 4, 5 and 6) for  $Fe_8$  systems respectively. Once the  $z$ -axis ( $\vec{z}$ ) of the ion is fixed, then  $\vec{x}$  is obtained by Gram-Schmidt orthogonalization procedure. Though the choice of this vector is arbitrary in a plane perpendicular to  $z$ -axis, we have fixed the direction of  $\vec{x}$  such as to have maximum projection along a  $M-O$  ( $M=Mn$ ,  $Fe$ ) bond in  $Mn_{12}Ac$

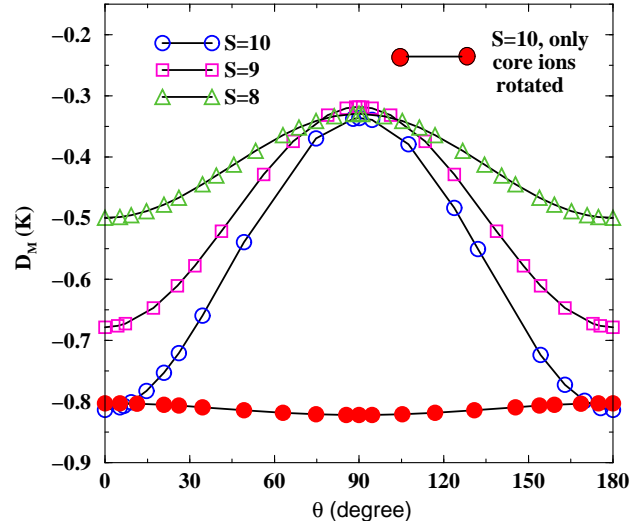


FIG. 6: Variation of  $D_M$  as a function of  $\theta$ , the angle the  $z$ -component of local anisotropy of  $Mn(III)$  ions makes with the laboratory  $Z$ -axis for scheme 2, in eigenstates with total spin 10, 9 and 8. The orientation of  $Mn(IV)$  ions is kept fixed at  $\sim 48^\circ$  from the molecular  $Z$ -axis. The curve with filled circles correspond to the variation of  $D_M$ , when the local anisotropies of the core  $Mn(IV)$  ions only are rotated and those of  $Mn(III)$  ions are fixed along the  $Z$  axis.

as well as in  $Fe_8$  (Fig. 2 and Fig. 10). If  $\vec{O}$  is the vector connecting a  $M$  site and a neighbouring  $O$  ion, then we obtain  $\vec{x}$  from,

$$\vec{x} = \vec{O} - (\vec{O} \cdot \vec{z}) \vec{z} \quad (8)$$

Then, the  $y$ -axis of the ion is obtained by taking cross product of the  $\vec{z}$  and  $\vec{x}$ ,  $\vec{y} = \vec{z} \times \vec{x}$ . These three mutually orthogonal vectors are then normalized to obtain the orthonormal set of coordinate axes  $x$ ,  $y$  and  $z$  of the ion centre. The single ion local axes is represented in the laboratory frame as,

$$\begin{aligned} x &= C_{i,Xx}X + C_{i,Yx}Y + C_{i,Zx}Z \\ y &= C_{i,Xy}X + C_{i,Yy}Y + C_{i,Zy}Z \\ z &= C_{i,Xz}X + C_{i,Yz}Y + C_{i,Zz}Z \end{aligned} \quad (9)$$

where,  $C_i$ s are the direction cosines of Eq. 7 and the index  $i$  correspond to the site  $i$ . The procedure is repeated for every magnetic ion to obtain coordinate axes set  $x$ ,  $y$  and  $z$  and the direction cosines in each case. We have obtained the magnetic anisotropy parameters  $D_M$  and  $E_M$  for  $Mn_{12}Ac$  and  $Fe_8$  clusters as a function of the angle of rotation of the local  $z$ -axis with respect to the laboratory  $Z$ -axis. In the following subsections, we discuss the results for the two clusters.

#### A. Magnetic anisotropy in $Mn_{12}Ac$ SMM

We have first obtained the ground state and few excited states of the  $Mn_{12}Ac$  system by exactly solving the

TABLE I:  $D_M$  values of ground and excited states of  $Mn_{12}Ac$  under various schemes in K. For scheme 2, we have presented the  $D_M$  values only for  $\theta=26.2^\circ$  for which the  $D_M$  value of the ground state matches with the experimentally observed value.

State	D <sub>M</sub> (K)		
	Scheme 1	Scheme 2	Scheme 3
Ground state (S=10)	-0.8028	-0.7209	0.3991
First excited state (S=9) $E_g=35.1$ K	-0.6722	-0.6105	0.3341
Second excited state (S=8) $E_g=60.4$ K	-0.5009	-0.4664	0.2488

unperturbed Hamiltonian given in Eq. 3, using the exchange interactions shown in Fig. 1 [9]. The ground state of the system corresponds to total spin 10 with a total spin 9 excited state at 35.1 K from the ground state. The second excited state occurs at 60.4 K from the ground state and corresponds to total spin 8. To obtain the molecular anisotropy values in these eigenstates, we have used different single-ion axial anisotropy values of -5.35 K and 1.226 K respectively for  $Mn(III)$  and  $Mn(IV)$  ions. We have also introduced transverse anisotropy of 0.022 K and 0.043 K for  $Mn(III)$  and  $Mn(IV)$  sites respectively. We have studied the variation of molecular anisotropy as a function of orientation of the local anisotropies by rotating the local  $\mathcal{D}$  tensor around the molecular  $Z$ -axis. Scheme 1 shown in Fig. 3 corresponds to the case when all the single-ion  $z$  axes are pointed parallel to the laboratory  $Z$  direction. In scheme 2 (Fig. 5), we have fixed the orientation of the local anisotropies of the core  $Mn(IV)$  ions along the line joining the ion and the molecular centre ( $\sim 48^\circ$  from the laboratory  $Z$ -axis), while the anisotropies of the  $Mn(III)$  ions is rotated and the angle which it makes with the molecular  $Z$ -axis is defined as  $\theta$  (refer Fig. 4). The orientation of the local anisotropy of  $Mn(III)$  ions for which we get the best agreement with experiments corresponds to  $\theta = 26^\circ$ . In scheme 3 (Fig. 5), we have restricted the  $z$ -component of single-ion anisotropy to the laboratory  $X - Y$  plane. We have studied the variation in the molecular anisotropies in these schemes for ground and the excited eigenstates. We show in Table I, the  $D_M$  values for the ground and the excited spin states of the molecule for schemes 1, 2 and 3. We note that when the local anisotropies are systematically varied, there is a very large variation in the molecular anisotropy as a function of the local orientation (Fig. 6). This seems to be true for all the states of  $Mn_{12}Ac$  we have studied. We note that given the orientations of local anisotropies, the actual molecular anisotropy values are different in different spin eigenstates. This may be rationalized from the fact that the energy gaps between the ground and the excited states are large as a consequence of which the spin correlations in these states are very different. We also note that in all cases, from the eigenvectors of the  $\mathcal{D}^{(M)}$  matrix, we find that the choice of our laboratory frame is very close to the principal axis

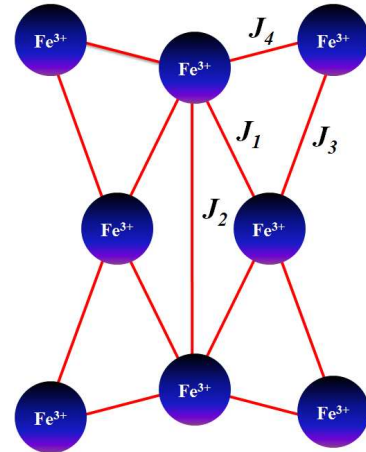


FIG. 7: Schematic of exchange interactions in  $Fe_8$  SMM. Js are the strength of superexchange interaction with  $J_1=150$  K,  $J_2=25$  K,  $J_3=30$  K,  $J_4=50$  K [9].

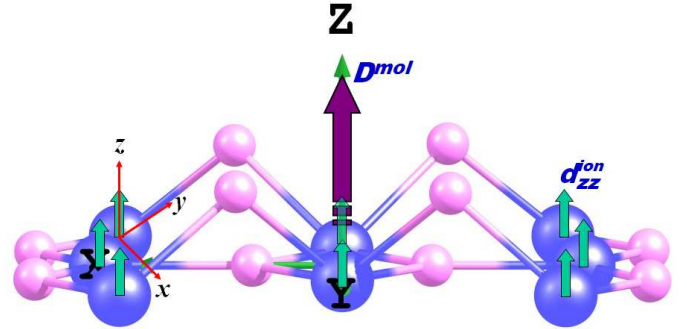


FIG. 8: Schematic diagram showing the directions of local anisotropy in  $Fe_8$ . The single-ion anisotropies of all the  $Fe(III)$  ions are directed along the laboratory  $Z$  axis (Scheme 4).

of the molecular system.

We also examined the role of magnetic orientations of the core  $Mn(IV)$  ions ( $s=3/2$ ) and the crown  $Mn(III)$  ions ( $s=2$ ) in determining the molecular anisotropies by fixing the single ion orientation of the crown  $Mn(III)$  ions at  $0^\circ$  and rotating only the orientation of the core  $Mn(IV)$  ions systematically. The variation of  $D_M$  for the S=10 ground state as a function of rotation of the local anisotropies of the core  $Mn(IV)$  ions is shown in Fig. 6. We find that the molecular anisotropy is not sensitive to the local orientations of the core  $Mn(IV)$  ions while the orientation of the crown  $Mn(III)$  ions control the variation of the molecular magnetic anisotropy in  $Mn_{12}Ac$ . It should be noted that, in the case of  $Mn_{12}Ac$ ,  $E_M$  vanishes by virtue of the  $D_{2d}$  point group symmetry to which the molecule belongs.

## B. Magnetic anisotropy in $Fe_8$ SMM

We have also computed the values of molecular anisotropy for the  $Fe_8$  molecular magnet. The unperturbed Hamiltonian in Eq. 3 is exactly solved using exchange parameters,  $J_1=150$  K,  $J_2=25$  K,  $J_3=30$  K,  $J_4=50$  K (Fig. 7) [9]. The ground state of the system corresponds to total spin  $S=10$  with a  $S=9$  state at 13.56 K, a  $S=9$  state at 27.28 K and a  $S=8$  state at 28.33 K above the ground state. To calculate the magnetic anisotropy of  $Fe_8$ , we have taken the single ion axial and rhombic anisotropy values for  $Fe(III)$  centers to be 1.96 K and 0.008 K respectively. Using these, we have computed the molecular anisotropy values for three schemes (Schemes 4, 5 and 6) shown in Fig. 8, 9 and 10. Scheme 4 corresponds to the case wherein the single-ion anisotropy of all the  $Fe(III)$  ions are pointed along the laboratory  $Z$  direction. In scheme 5, the anisotropies of the  $Fe(III)$  ions are inclined at an angle  $\theta$  to the laboratory  $Z$ -axis (refer Fig. 9). In Scheme 6, we have restricted the  $z$ -component of single-ion anisotropy to the laboratory  $X-Y$  plane. We have studied the variation in the molecular anisotropies as a function of orientation of local anisotropy in these schemes for ground and the excited eigenstates (Fig. 11). We show in Table II, the  $D_M$  values for the ground and the excited spin states of the molecule for schemes 4, 5 and 6. We note that when the local anisotropies are systematically varied, there is a very large variation in the molecular anisotropy as a function of the local orientation (Fig. 11), similar to  $Mn_{12}Ac$ , in all the eigenstates that we have studied. We also note that given the orientations of local anisotropies, the actual molecular anisotropy values are not very different in different spin eigenstates, since the energy gaps between the ground and the excited states are small and since the spin correlations in these states are not significantly different. The orientation of the local anisotropy centers for which we get the best agreement with experiments ( $D_M = -0.28$  K) corresponds to  $\theta \sim 99^\circ$  [22, 23]. As with  $Mn_{12}Ac$ , we find that the laboratory frame we have chosen is very close to molecular axis in all the cases. In case of  $Fe_8$  cluster, the  $D_2$  symmetry commutes with the Hamiltonian in Eq. 2 and allows for a non-zero  $E_M$  term. The variation of  $E_M$  as a function of  $\theta$  is shown in Fig. 12, the value of  $E_M$  for which  $D_M$  has the best fit is 0.017 K compared to the experimental estimate of 0.046 K obtained from High-frequency EPR measurements [19].

## IV. CONCLUSIONS

In this paper we presented a general method to calculate the molecular magnetic anisotropy parameters,  $D_M$  and  $E_M$  for single molecule magnets in a chosen eigenstate of the exchange Hamiltonian. Since, anisotropy is generally weak in SMMs compared to exchange interaction, we treat the anisotropy Hamiltonian as a perturbation over the exchange Hamiltonian. Calculation of

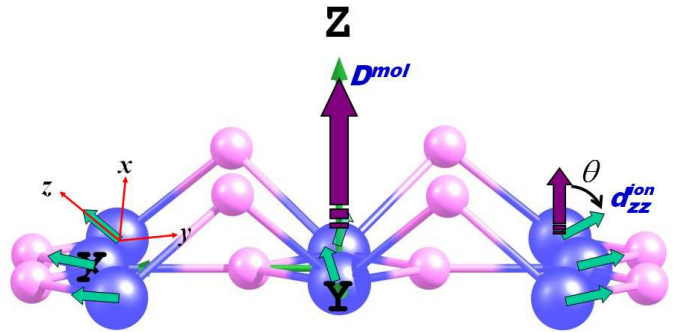


FIG. 9: Schematic diagram showing the directions of local anisotropy in  $Fe_8$ . The  $z$ -component of the single-ion anisotropies of all the  $Fe(III)$  ions are inclined at an angle  $\theta$  to the laboratory  $Z$  axis (Scheme 5).

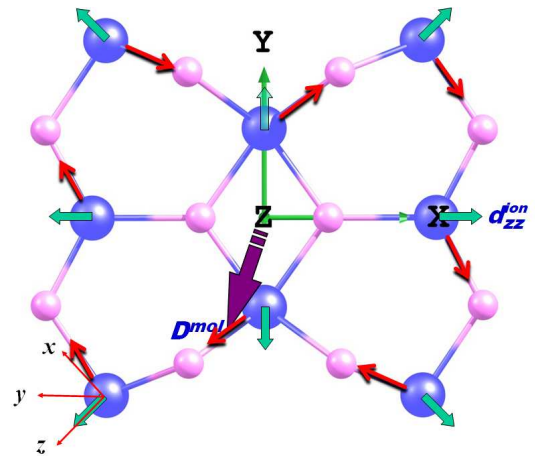


FIG. 10: Schematic diagram showing the directions of local anisotropy in  $Fe_8$ . The  $z$ -component of the single-ion anisotropies of all the  $Fe(III)$  ions are directed along the plane perpendicular to the laboratory  $Z$  axis (Scheme 6). The arrows indicate the  $Fe-O$  bonds on which the chosen local  $x$ -axis has maximum projection.

TABLE II:  $D_M$  values of ground and excited states of  $Fe_8$  under schemes 4, 5 and 6 in K. For scheme 5, we have presented the  $D_M$  values only for  $\theta=98.78^\circ$  for which the  $D_M$  value of the ground state matches with the experimentally observed value.

State	D <sub>M</sub> (K)		
	Scheme 4	Scheme 5	Scheme 6
Ground state ( $S=10$ )	0.6030	-0.2892	-0.3034
First excited state ( $S=9$ ) $E_g=13.56$ K	0.5821	-0.2783	-0.2923
Second excited state ( $S=9$ ) $E_g=27.28$ K	0.5877	-0.2797	-0.2952
Third excited state ( $S=8$ ) $E_g=28.33$ K	0.5503	-0.2694	-0.2758

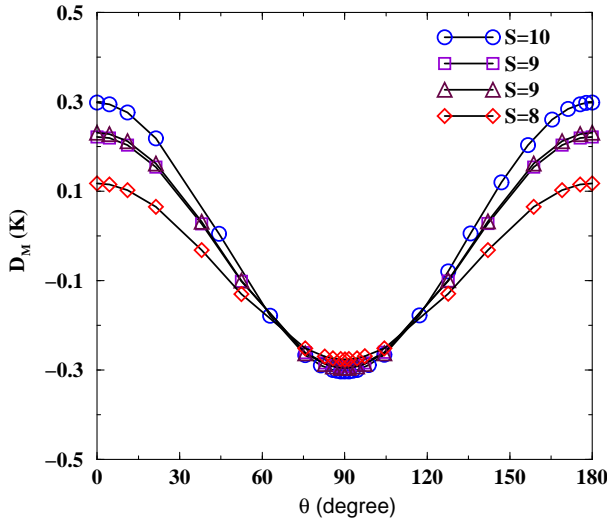


FIG. 11: Variation of  $D_M$  in  $Fe_8$  cluster as a function of  $\theta$ , the angle the  $z$ -component of local anisotropy of  $Fe(III)$  ions makes with the laboratory  $Z$ -axis for scheme 5.

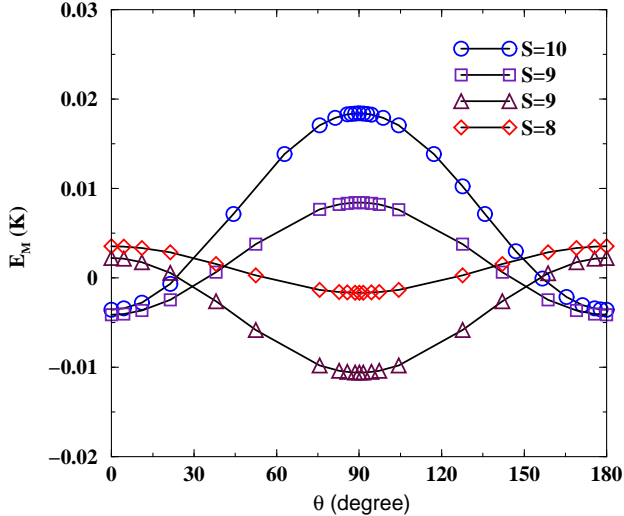


FIG. 12: Variation of  $E_M$  in  $Fe_8$  cluster as a function of  $\theta$ , the angle the  $z$ -component of local anisotropy of  $Fe(III)$  ions makes with the laboratory  $Z$ -axis for scheme 5.

$D_M$  and  $E_M$  values assuming only dipolar interactions between the transition metal ions give negligible values

of molecular magnetic anisotropy compared to the experimental values. Therefore, we focus on the molecular anisotropy from the single-ion anisotropies of the individual transition metal centers in the SMM. The single-ion anisotropy has relativistic origin, (spin-orbit interactions generally dominate over dipolar interactions between unpaired electrons in case of transition metal ions) and are hence short ranged with inverse cube dependence on distance. Therefore, we neglect interaction between spin moment on one ion with the orbital moment on another. This approximation simplifies the perturbation Hamiltonian. The molecular anisotropies are computed from the single-ion anisotropies, using first order perturbation theory for different spin states of the SMMs. We have computed the molecular magnetic anisotropy parameters of  $Mn_{12}Ac$  and  $Fe_8$  SMMs in various eigenstates of different total spin. We also studied the variation of molecular anisotropy by rotating the local anisotropy of the metal ions. In case of  $Mn_{12}Ac$ , we find that the molecular anisotropy changes drastically with the local anisotropy direction. The  $D_M$  value is different in ground and excited states we have computed, owing to large difference in spin-spin correlation values. The molecular anisotropy of  $Mn_{12}Ac$  does not change significantly with the orientation of the local anisotropy of the core Mn(IV) ions. In the case of  $Fe_8$  cluster also, we find that the molecular anisotropy parameters depend strongly on the orientation of the local anisotropy.  $D_M$  value is not very different in ground and excited states probably due to small energy gaps which implies similar spin-spin correlations. In case of  $Mn_{12}Ac$ , the first order rhombic anisotropy term is zero due to the  $D_{2d}$  symmetry of the molecule while it is non-zero in  $Fe_8$ . The second order rhombic anisotropy terms commute with the molecular symmetry of the  $Mn_{12}Ac$  cluster and cause tunneling between the states on either side of the double potential well. Our method can also be extended to the calculation of these anisotropy constants.

### Acknowledgments

The authors thank Indo-French Centre for Promotion of Advanced Research (IFCPAR) under the project 3108-3 and Indo-Swedish Research Council under the project VT-SK001 for the financial support.

---

[1] L. Thomas, F. Lioni, R. Ballou, D. Gatteschi, R. Sessoli, and B. Barbara, *Nature* **383**, 145 (1996).

[2] W. Linert and M. Verdaguer, *Molecular Magnets: Recent Highlights* (Springer-Verlag, New York, 2003).

[3] J. S. Miller and M. Drillon, *Magnetism: Molecules to Materials IV* (Wiley-VCH Verlag GMBH, 2003).

[4] M. Shoji, K. Koizumi, T. Hamamoto, Y. Kitagawa, S. Yamanaka, M. Okumura, and K. Yamaguchi, *Chem. Phys. Lett.* **421**, 483 (2006).

[5] K. Wieghardt, K. Pohl, I. Jibril, and G. Huttner, *Angew. Chem. Int. Ed. Engl.* **24**, 77 (1984).

[6] E. D. Barco, N. Vernier, J. M. Hernandez, J. Tejada, E. M. Chudnovski, E. Molins, and G. Bellessa, *Euro. Phys. Lett.* **47**, 722 (1999).

[7] R. Sessoli, D. Gatteschi, A. Canneschi, and M. A. Novak, *Nature* **365**, 141 (1993).

- [8] S. Sahoo, R. Rajamani, S. Ramasesha, and D. Sen, arXiv:0804.1319 (2008).
- [9] C. Raghu, I. Rudra, D. Sen, and S. Ramasesha, Phys. Rev. B **64**, 064419 (2001).
- [10] S. Sinnecker and F. Neese, J. Phys. Chem A **110**, 12267 (2006).
- [11] T. Baruah and M. R. Pederson, Chem. Phys. Lett. **360**, 144 (2002).
- [12] J. R. Arino, T. Baruah, and M. R. Pederson, J. Chem. Phys. **123**, 044303 (2005).
- [13] J. L. Oudar and J. Zyss, Phys. Rev. A **26**, 2016 (1982).
- [14] A. Bencini, C. Benelli, and D. Gatteschi, Coord. Chem. Rev. **60**, 131 (1984).
- [15] A. Bencini and D. Gatteschi, *EPR of Exchange Coupled Systems* (Springer, Berlin, 1990).
- [16] A. Carrington and A. McLachlan, *Introduction to Magnetic Resonance: with applications to chemistry and chemical physics* (Harrer and Row Publishers, New York, 1967).
- [17] S. Ramasesha and Z. G. Soos, Chem. Phys. **91**, 35 (1984).
- [18] A. L. Barra, D. Gatteschi, and R. Sessoli, Chem. Eur. J. **6**, 1608 (2000).
- [19] A.-L. Barra, P. Debrunner, D. Gatteschi, C. E. Schulz, and R. Sessoli, Europhys. Lett. **35**, 133 (1996).
- [20] A. Cornia, R. Sessoli, L. Sorace, D. Gatteschi, A. L. Barra, and C. Daiguebonne, Phys. Rev. Lett. **89**, 257201 (2002).
- [21] A. L. Barra, D. Gatteschi, R. Sessoli, G. L. Abbati, A. Cornia, A. C. Fabretti, and M. G. Uytterhoeven, Angew. Chem. Int. Ed. Engl. **36**, 2329 (1997).
- [22] S. Accorsi, A.-L. Barra, A. Caneschi, G. Chastanet, A. Cornia, A. Fabretti, D. Gatteschi, C. Mortalo, E. Olivieri, F. Parenti, et al., J. Am. Chem. Soc. **128**, 4742 (2006).
- [23] P. t. Heerdt, M. Stefan, E. Goovaerts, A. Canneschi, and A. Cornia, J. Mag. Res. **179**, 29 (2006).